Hydrolysis of the 5′-*p*-Nitrophenyl Ester of TMP by the Proofreading Exonuclease (ε) Subunit of *Escherichia coli* DNA Polymerase III†

Samir Hamdan, Esther M. Bulloch, Phillip R. Thompson, Jennifer L. Beck, Ji Yeon Yang, Jeffrey A. Crowther, Penelope E. Lilley, Paul D. Carr, David L. Ollis, Susan E. Brown, and Nicholas E. Dixon*

Research School of Chemistry, Australian National University, Canberra, ACT 0200, Australia

Received November 14, 2001; Revised Manuscript Received February 11, 2002

ABSTRACT: The core of DNA polymerase III, the replicative polymerase in *Escherichia coli*, consists of three subunits (α, ε, and θ). The ε subunit is the 3′−5′ proofreading exonuclease that associates with the polymerase (α) through its C-terminal region and θ through a 185-residue N-terminal domain (ε186). A spectrophotometric assay for measurement of ε activity is described. Proteins ε and ε186 and the ε186·θ complex catalyzed the hydrolysis of the 5′-*p*-nitrophenyl ester of TMP (*p*NP-TMP) with similar values of k_{cat} and K_M, confirming that the N-terminal domain of ε bears the exonuclease active site, and showing that association with θ has little direct effect on the chemistry occurring at the active site of ε. On the other hand, formation of the complex with θ stabilized ε186 by ∼14 °C against thermal inactivation. For ε186, $k_{cat} = 293$ min^{-1} and $K_M = 1.08$ mM at pH 8.00 and 25 °C, with a Mn^{2+} concentration of 1 mM. Hydrolysis of *p*NP-TMP by ε186 depended absolutely on divalent metal ions, and was inhibited by the product TMP. Dependencies on Mn^{2+} and Mg^{2+} concentrations were examined, giving a K_{Mn} of 0.31 mM and a k_{cat} of 334 min^{-1} for Mn^{2+} and a K_{Mg} of 6.9 mM and a k_{cat} of 19.9 min^{-1} for Mg^{2+}. Inhibition by TMP was formally competitive [$K_i = 4.3\,\mu$M (with a Mn^{2+} concentration of 1 mM)]. The pH dependence of *p*NP-TMP hydrolysis by ε186, in the pH range of 6.5−9.0, was found to be simple. K_M was essentially invariant between pH 6.5 and 8.5, while k_{cat} depended on titration of a single group with a pK_a of 7.7, approaching limiting values of 50 min^{-1} at pH <6.5 and 400 min^{-1} at pH >9.0. These data are used in conjunction with crystal structures of the complex of ε186 with TMP and two Mn(II) ions bound at the active site to develop insights into the mechanisms of *p*NP-TMP hydrolysis by ε at high and low pH values.

Since its discovery nearly 25 years ago, the *Escherichia coli* DNA polymerase III (pol III)[1] holoenzyme has been studied extensively as a model replication machine (*1*−*3*). The 10 different protein subunits of the holoenzyme function in cooperation with other replication proteins to carry out the duplication of the entire *E. coli* chromosome with astonishing efficiency, processivity, and fidelity. The core of pol III contains three subunits. The 130 kDa α subunit includes the polymerase active site. The ε subunit (28 kDa), encoded by the *dnaQ* gene (*4*−*11*), is the 3′−5′ proofreading exonuclease, while the 9 kDa θ subunit (*12*) has no known discrete function. The separation of the polymerase and exonuclease activities of pol III between different subunits is in contrast to many DNA polymerases where both activities are present on a single polypeptide chain (*13*−*15*).

The ε subunit is itself composed of two distinct domains (*16*−*18*). The N-terminal domain (codons 2−186 of *dnaQ*, ε186) contains the exonuclease active site and the binding site for θ, while the small C-terminal domain (within codons 187−243) contains the α binding site (*16*, *17*). Since ε interacts with both α and θ, it is likely to play an important structural role within the pol III core (*12*, *16*, *17*). Intersubunit interactions also influence enzymatic activities; for example, interaction of α and ε was reported to stimulate the exonuclease activity of ε on DNA substrates between 10- and 80-fold and the polymerase activity of α 2-fold (*19*), while θ stimulated the activity of ε on DNA substrates ∼2−4-fold (*12*, *17*). Moreover, assembly of a highly processive pol III holoenzyme requires the presence of ε in its core (*14*, *20*).

Amino acid alignments of 3′−5′ exonuclease domains or subunits of prokaryotic and eukaryotic DNA polymerases with the corresponding domain in the X-ray crystal structure of the large (Klenow) proteolytic fragment of DNA polymerase I (pol I) (*21*) have identified several conserved motifs (Exo I, Exo II, and Exo III) (*22*, *23*). In ε and some other proofreading exonucleases, the Exo III motif is substituted with an alternative motif called Exo IIIε, which contains at least three amino acids essential for the exonuclease activity (*18*, *24*, *25*). The analysis of *dnaQ* mutants has confirmed the importance of the three core motifs in the catalytic activity of ε (*26*−*28*), and it has been shown that the isolated N-terminal domain is active as an exonuclease (*17*, *18*).

† This work was supported in part by an Australian Postgraduate Research Award (to P.R.T.) and an Australian Research Council Australian Postdoctoral Fellowship (to S.E.B.).

* To whom correspondence should be addressed. Telephone: +61-2-6125 4391. Fax: +61-2-6125 0750. E-mail: dixon@rsc.anu.edu.au.

[1] Abbreviations: DTT, dithiothreitol; ε186, N-terminal domain of the ε subunit of *E. coli* DNA polymerase III; *p*NP-TMP, 5′-*p*-nitrophenyl ester of thymidine 5′-monophosphate; pol I, *E. coli* DNA polymerase I; pol III, *E. coli* DNA polymerase III; ssDNA, single-stranded DNA.

10.1021/bi0159480 CCC: $22.00
Published on Web 03/27/2002

Scheme 1: Hydrolysis of Thymidine 5′-Monophosphate *p*-Nitrophenyl Ester (*p*NP-TMP) to TMP and *p*-Nitrophenol, Promoted by the ϵ Subunit of DNA Polymerase III

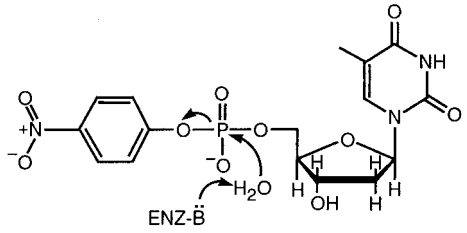

Although the structure of the full-length ϵ subunit is still unknown, a model for the structure of ϵ186 has recently been derived from a combination of NMR spectroscopy and molecular modeling (*29*), and its X-ray structure has been determined at 1.7 Å resolution (*25*).

The exonuclease activity of ϵ and other proofreading exonucleases has usually been monitored using radiolabeled ssDNA or primer−template substrates that have mismatched termini (*11*, *17*, *19*, *30*−*32*). As an alternative approach to understanding fine details of the mechanism of action of ϵ, we investigated the use of a noncanonical nucleoside 5′-phosphodiester substrate, the *p*-nitrophenyl ester of thymidine 5′-monophosphate (*p*NP-TMP; Scheme 1). Hydrolysis of such a small compound should not be influenced by the extensive interactions in and around the active site expected for polynucleotide substrates. Thus, comparison of its enzyme-catalyzed hydrolysis with that of DNA substrates should allow the contributions of these more extensive peripheral interactions to be separated from those due to the active site residues that actually participate in the chemistry.

Because hydrolysis of *p*NP-TMP to *p*-nitrophenol and TMP can be monitored spectrophotometrically, it also provides a continuous, convenient, and reproducible assay for measuring the rates of nucleotide phosphodiester hydrolysis by ϵ. We used this assay to confirm previous results, in particular, that the N-terminal domain of ϵ is responsible for the exonuclease activity. It was further shown that although the thermal stability of ϵ186 is increased very substantially by formation of its complex with θ, the complex is just a little less active in *p*NP-TMP hydrolysis than ϵ186 alone. Hydrolysis rates were also dependent on the presence of metal ion cofactors such as Mn^{2+} and Mg^{2+}, and were inhibited by TMP, a nucleotide product of the exonuclease reaction. We also examined the pH dependence of Michaelis−Menten parameters for the ϵ186-catalyzed hydrolysis of *p*NP-TMP. These data, in conjunction with the recently determined crystal structures of the active site in complex with two Mn(II) ions and TMP at low and high pH (*25*), give interesting insights into the mechanism of substrate hydrolysis by ϵ.

EXPERIMENTAL PROCEDURES

Protein Expression and Purification. Details of the construction of plasmids that direct expression of ϵ and ϵ186, as well as methods adapted from published procedures for the isolation of purified samples of ϵ (*11*, *32*), ϵ186 (*18*), θ (*33*), and the ϵ186·θ complex (*17*), and their physical characterization by SDS−PAGE and ESI-MS, are given in the Supporting Information. As judged by these analyses, ϵ186 and the ϵ186·θ complex were obtained in a highly purified form, while the sample of ϵ was contaminated to the extent of ∼20% by other proteins. Concentrations of freshly dialyzed purified samples of ϵ, ϵ186, θ, and the ϵ186·θ complex were determined spectrophotometrically at 280 nm, using ϵ_{280} values of 12 090, 6400, 8250, and 14 650 M^{-1} cm^{-1}, respectively (*34*). Samples for assays were diluted when necessary in 20 mM Tris·HCl (pH 7.6), 2 mM DTT, 0.5 mM EDTA, and 10% (w/v) glycerol (buffer C) containing 0.1 M NaCl.

Reagents. The sodium salts of *p*NP-TMP and TMP were used as received from Sigma. Stock solutions were prepared in 50 mM Tris·HCl (pH 8.00) and 150 mM NaCl and stored frozen in small aliquots at −20 °C. Their concentrations were determined spectrophotometrically, using an ϵ_{270} of 16 250 M^{-1} cm^{-1} for *p*NP-TMP (*35*) and an ϵ_{267} of 9600 M^{-1} cm^{-1} for TMP. Reverse phase HPLC using an analytical C18 column was used to show that stocks of *p*NP-TMP were not contaminated by TMP (<0.1%). Columns were developed at 1 mL/min using a linear gradient from 10 to 70% methanol in 50 mM sodium acetate buffer (pH 5) over the course of 20 min. TMP, *p*NP-TMP, and *p*-nitrophenol eluted in that order, and were well separated.

Spectrophotometric Activity Assays. The activities of samples of ϵ, ϵ186, and the ϵ186·θ complex were determined spectrophotometrically by monitoring the production of *p*-nitrophenolate anion produced by hydrolysis of *p*NP-TMP at 420 nm (Scheme 1), using a Cary model 1 spectrophotometer with the cuvette chamber thermostated at 25 °C. For routine assays, a stock solution of *p*NP-TMP was diluted with assay buffer [50 mM Tris·HCl (pH 8.00), 150 mM NaCl, and 1 mM DTT, to 970−980 μL] to a final concentration of 3.0 mM in a 1 mL quartz cuvette. Following equilibration at 25 °C, solutions of $MnCl_2$ (10 μL) and enzyme (10−20 μL) were added to give final concentrations of 1 mM and 100−400 nM, respectively. The solution was quickly and thoroughly mixed with a bent glass rod, and changes in A_{420} were followed over several minutes. Routine assays were generally carried out in duplicate, and initial rates (v_0) were estimated as tangents to curves of A_{420} versus time at zero time, using the Cary-WinUV software (version 2.00). Rates of *p*NP-TMP hydrolysis were calculated using a value of 12 950 M^{-1} cm^{-1} for the ϵ_{420} of *p*-nitrophenol at pH 8.00.

The dependence of v_0 on enzyme concentration ($[E]_0$) was determined for concentrations of ϵ186 in the range of 0−700 nM, under routine assay conditions. Estimates of Michaelis−Menten parameters were obtained from data measured at *p*NP-TMP concentrations ($[S]_0$) in the range of 0.2−5.2 mM where $[Mn^{2+}] = 1$ mM and $[S]_0 = 1.5$−12 mM where $[Mg^{2+}] = 12$ mM. Values of K_M and k_{cat} were generally calculated by linear least-squares analysis of Hanes−Woolf plots ($[S]_0/v_0$ vs $[S]_0$). The effect of divalent metal ions on the rate of reaction was studied with $[Mg^{2+}] = 0.5$−12 mM and $[S]_0 = 12$ mM, or $[Mn^{2+}] = 0.05$−1.2 mM and $[S]_0 = 3.0$ mM. Product inhibition by TMP was studied by varying $[S]_0$ (0.4−4.2 mM) at each $[TMP]_0$ (0−8 μM), with $[Mn^{2+}] = 1$ mM. In this case, values of K_i for TMP inhibition and K_M and k_{cat} for substrate hydrolysis were obtained from a global nonlinear least-squares fit of data to equations describing competitive inhibition, using the program Dynafit (*36*).

Thermal stabilities of ϵ186 and the ϵ186·θ complex were measured as follows. Enzyme samples (32 and 13 μM,

respectively) in assay buffer containing 100 μM $MnCl_2$ were treated at various temperatures between 35.0 and 59.5 °C for exactly 10 min, and then cooled in ice. Samples (10 μL) were taken, and residual activities were determined by assay under the routine assay conditions.

pH Dependence of pNP-TMP Hydrolysis by ϵ186. Values of k_{cat} and K_M at each pH value were determined essentially as described above from assays carried out at appropriate concentrations of ϵ186, at 25 °C in 50 mM buffer solutions [Na·MES (pH 6.52) or Tris·HCl (pH 7.01−8.95)] containing 150 mM NaCl, 1 mM DTT, and 1 mM $MnSO_4$, except that 3 mM $MgSO_4$ was used at pH 6.52. For assays at each pH value, a stock solution of *p*NP-TMP (227 mM, in 150 mM NaCl) was first diluted 5-fold in the particular assay buffer, and then suitable volumes of this solution were used to give a $[S]_0$ in the range of 0.4−4.2 mM. The absence of buffer catalysis was established in preliminary assays at two or more different buffer concentrations. Concentrations of *p*-nitrophenol were determined using an ϵ_{420} of 14 365 M^{-1} cm^{-1} for *p*-nitrophenolate anion and the measured pK_a of 7.04 for *p*-nitrophenol under these conditions.

RESULTS

Hydrolysis of pNP-TMP by ϵ, ϵ186, and the ϵ186·θ Complex. Initial spectrophotometric experiments established that ϵ and ϵ186 could both promote release of *p*-nitrophenol from the substrate *p*NP-TMP, and stoichiometric quantities of the products TMP and *p*-nitrophenol were separated and identified by HPLC, as described in Experimental Procedures. This suggests the mechanism of cleavage (Scheme 1) mimics the natural reaction promoted by ϵ, where the TMP moiety is a 3′-mismatched terminal nucleotide, and the leaving group *p*-nitrophenolate substitutes for the remainder of the polynucleotide chain (*31*). The rate of change of A_{420} was used to determine the initial velocity of the hydrolysis reaction (v_0). In general, the rates decreased significantly with time (not shown). Most likely, this reflects inhibition of the enzymes by the strongly binding product inhibitor TMP (see below). Initial rates estimated simply from tangents to the curves at time zero were reproducible to within ±5%.

In preliminary studies using full-length ϵ as the enzyme (*37*), we first showed that the initial rate of ϵ-catalyzed *p*NP-TMP hydrolysis (at a particular substrate concentration) reached a maximum at pH ∼8. Although initial rates at pH 8 were unaffected by the buffer that was used (HEPES and Tris gave identical rates), they were stimulated ∼2-fold (relative to buffer alone at pH 8.0) by 0.5 M sodium chloride, and *p*NP-TMP hydrolysis by ϵ was shown to be absolutely dependent on the presence of a divalent metal ion, Mn^{2+} being preferred over Mg^{2+}. After further measurements of the dependence of rates on $[p\text{NP-TMP}]_0$ and $[Mn^{2+}]$, conditions for routine assays (given in Experimental Procedures) were defined. Because full-length ϵ had been purified following its refolding from solutions in 3 M guanidinium chloride and has limited solubility (*29*), we chose to carry out most of the studies reported here on the isolated N-terminal domain, ϵ186. In contrast to ϵ, this domain is isolated in good yield from the soluble fraction following lysis of cells, by conventional chromatographic techniques (*18*).

The initial rate of *p*NP-TMP hydrolysis was proportional to $[\epsilon186]_0$ (Figure 1A) and also $[\epsilon]_0$ (not shown), over a 20-fold range of concentrations. Diluted samples of ϵ186 were found to be stable on storage in buffer C containing 100 mM NaCl for >12 h when kept at 0 °C.

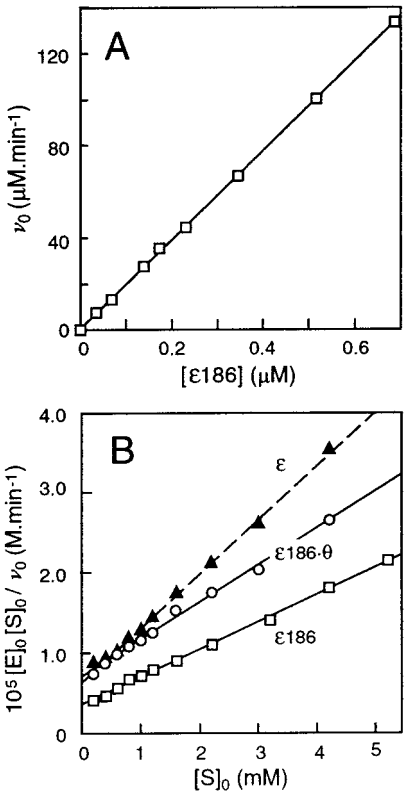

FIGURE 1: Hydrolysis of *p*NP-TMP by ϵ, ϵ186, and the ϵ186·θ complex, at pH 8.00 and 25 °C. (A) The rate of hydrolysis of *p*NP-TMP as a function of ϵ186 concentration. The concentration of *p*NP-TMP was 3.0 mM, and the concentration of $MnCl_2$ was 1 mM. (B) Hanes−Woolf plots, normalized for values of $[E]_0$, for the hydrolysis of *p*NP-TMP by ϵ, ϵ186, and the ϵ186·θ complex, showing the effect of *p*NP-TMP concentration on the rate of hydrolysis (1 mM $MnCl_2$). The experimental data points are shown, and the lines were calculated using values for K_M and k_{cat} determined by linear least-squares analysis, as follows: ϵ, K_M = 0.95 mM and k_{cat} = 148 min^{-1} (▲); ϵ186, K_M = 1.08 mM and k_{cat} = 293 min^{-1} (□); and ϵ186·θ, K_M = 1.51 mM and k_{cat} = 215 min^{-1} (○).

Initial rates of *p*NP-TMP hydrolysis promoted by ϵ, ϵ186, and the ϵ186·θ complex were determined under standard assay conditions [with 1 mM Mn^{2+} (pH 8.0)] at several *p*NP-TMP concentrations. The linearity of Hanes−Woolf plots (Figure 1B) confirmed that *p*NP-TMP hydrolysis followed Michaelis−Menten kinetics for all three enzymes. The kinetic parameters for the hydrolysis of *p*NP-TMP were as follows: K_M = 1.08 ± 0.05 mM and k_{cat} = 293 ± 4 min^{-1} for ϵ186 and K_M = 0.95 ± 0.05 mM and k_{cat} = 148 ± 3 min^{-1} for ϵ (Figure 1B). Thus, while values of K_M for the two enzymes were essentially identical, k_{cat} for ϵ186 was approximately twice that for full-length ϵ. While this difference is partly due to the presence of impurities in our preparation of ϵ, a similar difference (2.4-fold) between the two enzymes in their efficiency of hydrolysis of a ssDNA substrate has been noted previously (*17*). Nevertheless, it is clear that the N-terminal domain of ϵ is responsible for the hydrolysis of *p*NP-TMP, as has also been observed directly for its 3′−5′ exonuclease activity using a radiolabeled mismatched primer−template (*18*) and a partial duplex and ssDNA (*17*) as substrates.

The kinetic parameters for the ϵ186·θ complex (K_M = 1.51 ± 0.09 mM, k_{cat} = 215 ± 6 min^{-1}; Figure 1B) were also

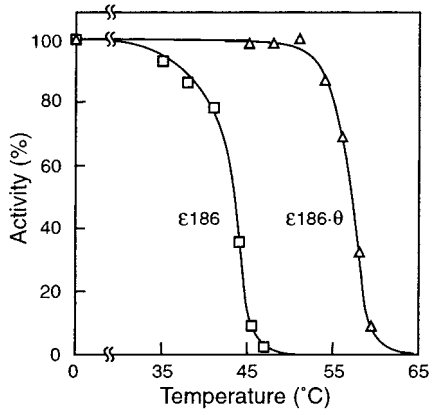

FIGURE 2: Thermostability of ϵ186 and the ϵ186·θ complex. *p*NP-TMP hydrolase activity (percentage of that of untreated samples) remaining after treatment of ϵ186 (□, 32 μM) and ϵ186.θ (△, 13 μM) in 50 mM Tris·HCl (pH 8.0), 150 mM NaCl, 1 mM DTT, and 100 μM $MnCl_2$ for 10 min at various temperatures.

similar to those for ϵ186, indicating that complexation with θ does not greatly affect the activity of ϵ186 in this assay. Nevertheless, the ~25% reduction in k_{cat} for ϵ186 on formation of the complex is probably significant, because it was reproduced with two independent preparations of the complex. When quantities of ϵ, ϵ186, and the ϵ186·θ complex corresponding to identical amounts of *p*NP-TMP hydrolase activity were electrophoresed through an SDS−polyacrylamide gel and stained with Coomassie Blue (see the Supporting Information), the minor differences in staining intensity among the ϵ and ϵ186 bands also indicated that the observed difference in k_{cat} probably reflects a real difference in the activities of the protein preparations.

Although formation of the complex with θ did not greatly affect the activity of ϵ186, it did markedly increase its thermal stability (Figure 2). The temperature at which 50% of the activity of the enzyme was irreversibly lost in 10 min was raised by some 14 °C from 43 to 57 °C by its interaction with θ.

Hydrolysis of pNP-TMP by ϵ186 Requires Divalent Metal Ions. In proofreading assays using $[dA]_{200}$·$[(dT)_{16}$-$([^3H]dC)_6]$ (*37*) and other substrates (*32*), it was found that ϵ had an absolute requirement for a divalent metal ion (usually Mg^{2+}) for phosphodiesterase activity. We found that with *p*NP-TMP as the substrate, rates were higher with Mn^{2+} than with Mg^{2+} at the same concentrations. Accordingly, the rate of hydrolysis of *p*NP-TMP by ϵ186 was measured as a function of both $[Mg^{2+}]$ and $[Mn^{2+}]$, and Hanes−Woolf plots were used to obtain estimates of k_{cat} and Michaelis constants for the metal ions. For Mn^{2+} ($[S]_0 = 3.0$ mM), $K_{Mn} = 0.31 \pm 0.03$ mM and $k_{cat} = 334 \pm 9$ min^{-1} (Figure 3A). Under similar conditions, Mg^{2+} could substitute, albeit poorly: when $[S]_0 = 3.0$ mM, $K_{Mg} = 9.4 \pm 1.3$ mM and $k_{cat} = 11.1 \pm 0.9$ min^{-1}; when $[S]_0 = 12.0$ mM, $K_{Mg} = 6.9 \pm 0.5$ mM and $k_{cat} = 19.9 \pm 0.7$ min^{-1} (Figure 3B). A study of the dependence of v_0 on $[S]_0$ with $[Mg^{2+}] = 12.0$ mM gave a K_M of 4.1 ± 0.4 mM for *p*NP-TMP and a k_{cat} of 18.9 ± 0.6 min^{-1} (not shown).

Noting that K_M for *p*NP-TMP and K_{Me} for the metal ions were each determined under conditions where concentrations of the other component were subsaturating, the values of k_{cat} underestimate the true maximum turnover number k_{cat}'. We have not attempted at this stage to carry out a complete

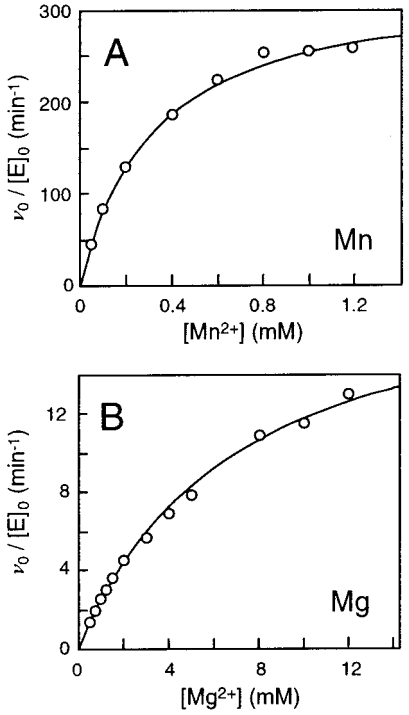

FIGURE 3: Dependence of ϵ186-promoted *p*NP-TMP hydrolysis on concentrations of $MnCl_2$ (A) and $MgCl_2$ (B), normalized by values of $[E]_0$. The solid lines were calculated from values of k_{cat} and K_{Me} derived by linear least-squares fitting of data in the form of Hanes−Woolf plots. (A) For Mn^{2+}, $[S]_0 = 3.0$ mM, $K_{Mn} = 0.3$ mM, and $k_{cat} = 334$ min^{-1}. (B) For Mg^{2+}, $[S]_0 = 12.0$ mM, $K_{Mg} = 6.9$ mM, and $k_{cat} = 19.9$ min^{-1}.

study of the dependence of K_{Mn} and K_{Mg} on $[S]_0$, or of K_M for *p*NP-TMP on metal ion concentrations. Given that the active site of ϵ in the crystal structure (*25*) contains two divalent metal ions that both participate in substrate binding as well as its hydrolysis (see the Discussion), it would be surprising if metal ion and substrate binding did not occur cooperatively. Nevertheless, estimates of maximum values of k_{cat}' can be made on the assumption of the independence of binding of *p*NP-TMP and the metal ions. For Mn^{2+}, these calculations give a k_{cat}' of 384 ± 14 min^{-1} (from k_{cat} for *p*NP-TMP at 1 mM Mn^{2+} and the value of K_{Mn} at $[S]_0 = 3.0$ mM) and a k_{cat}' of 454 ± 17 min^{-1} (from k_{cat} for Mn^{2+} at $[S]_0 = 3.0$ mM and K_M for *p*NP-TMP at 1 mM Mn^{2+}). Similar calculations for Mg^{2+} give a k_{cat}' of 30 ± 2 min^{-1} (from k_{cat} for *p*NP-TMP at 12 mM Mg^{2+} and the value of K_{Mg} at $[S]_0 = 12$ mM) and a k_{cat}' of 27 ± 2 min^{-1} (from k_{cat} for Mn^{2+} at $[S]_0 = 12$ mM and K_M for *p*NP-TMP at 12 mM Mn^{2+}).

Thus, k_{cat}' for Mg^{2+}-promoted *p*NP-TMP hydrolysis by ϵ186 is at least 12-fold lower than that for the Mn^{2+}-catalyzed reaction, while Mn^{2+} binds 20−30-fold more avidly than Mg^{2+} in the Michaelis complex with *p*NP-TMP. On the other hand, K_M for the substrate itself was only ~4-fold lower with Mn^{2+} than with Mg^{2+}.

Hydrolysis of pNP-TMP by ϵ186 Is Inhibited by TMP. It was known that the proofreading activity of ϵ, as measured with poly(dA)·$[(dT)_{18}$-$([^3H]dC)_{2.6-2.8}]_n$ (*11*) or $(dT)_{10}$ (*32*) as a substrate, is inhibited by nucleoside 5′-monophosphates, products of the reaction it catalyzes. A study of the effect of TMP on *p*NP-TMP hydrolysis by ϵ186 in the presence of 1 mM Mn^{2+} showed that TMP also inhibits this reaction. The

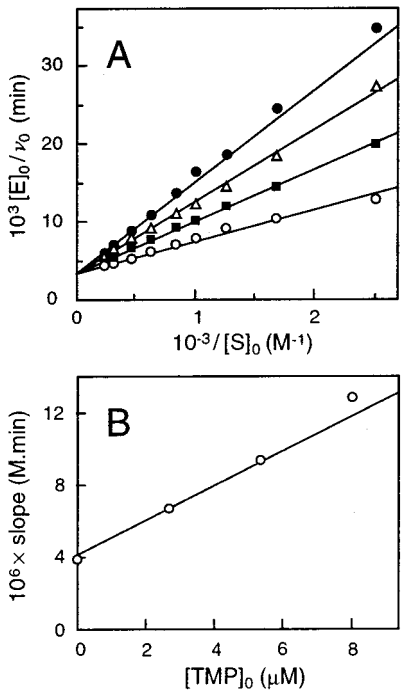

FIGURE 4: Competitive inhibition of ϵ186-promoted *p*NP-TMP hydrolysis by TMP. (A) Lineweaver−Burk plots showing TMP inhibition of the hydrolysis of *p*NP-TMP by ϵ186 (1 mM Mn^{2+}). Experimental points are shown: $[TMP]_0 = 0$ (○), 2.66 (■), 5.33 (△), and 7.99 μM (●). (B) Dependence of least-squares slopes of Lineweaver−Burk plots on $[TMP]_0$. The lines were calculated using a k_{cat} of 295 min^{-1}, a K_M of 1.20 mM, and a K_i of 4.3 μM, obtained using a competitive inhibition model in the program Dynafit (*36*).

data could be fit well to equations describing competitive inhibition with a k_{cat} of 295 ± 6 min^{-1}, a K_M of 1.20 ± 0.07 mM, and a K_i of 4.3 ± 0.3 μM (Figure 4). The value of K_i for TMP is thus almost 300-fold lower than the K_M for *p*NP-TMP under these conditions. It is also ~120-fold lower than that determined previously with ϵ using a DNA substrate in the presence of $MgCl_2$ at 5 mM (*32*). While this is undoubtedly in part due to more avid binding of the nucleotide inhibitor to Mn^{2+} than to Mg^{2+} at the active site of ϵ186, as is seen in the effect on K_M for *p*NP-TMP hydrolysis with Mn^{2+} (1 mM) versus Mg^{2+} (4 mM), it is also very likely that TMP is genuinely less effective in competing with DNA substrates that bind through more extensive interactions in and around the active site.

pH Dependence of Hydrolysis of pNP-TMP by ϵ186. Michaelis−Menten parameters describing hydrolysis of pNP-TMP by ϵ186 were determined from Hanes−Woolf plots of data measured in buffers at several pH values between 6.52 and 8.95. It was not possible to extend data to higher pHs because of precipitation of Mn ions. At all pH values, buffers contained $MnSO_4$ at concentrations that were shown to be near-saturating. A lack of a strong dependence of K_{Mn} on pH is expected from the structure of the active site (*25*), where all of the ligands that directly coordinate the metal ions are carboxylates, which should be deprotonated over the pH range examined here. Measured values of K_M for *p*NP-TMP were also essentially independent of pH over this range, though the upward trend at pH >8.5 (Figure 5B) may indicate a contribution to substrate binding by the protonated form of a strongly basic (e.g., arginine) residue.

Measured values of k_{cat} showed a strikingly simple dependence on pH, reflecting the titration of a single group

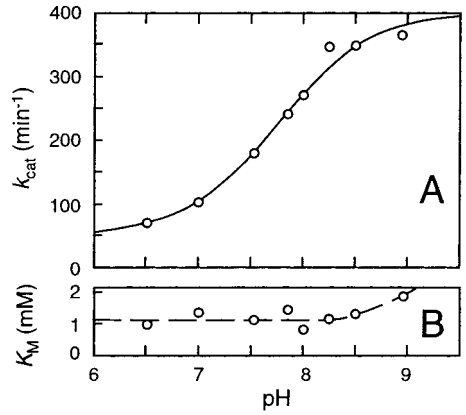

FIGURE 5: pH dependence of k_{cat} (A) and K_M (B) for ϵ186-promoted hydrolysis of *p*NP-TMP at 25 °C, where $[Mn^{2+}] = 1.0$ mM (except at pH 6.52, where $[Mn^{2+}] = 3.0$ mM). The kinetic parameters at each pH value were determined by linear least-squares fits of initial rates plotted as Hanes−Woolf plots. Buffers that were used were 50 mM Na·MES (pH 6.52) and 50 mM Tris·HCl (pH 7.01−8.95) containing 150 mM NaCl and 1 mM DTT. Standard errors in the estimates of K_M were less than ±12% and those for k_{cat} less than ±5%. The solid line in panel A was calculated according to the mechanism in Scheme 2, with a k_1 of 50 min^{-1}, a k_2 of 400 min^{-1}, and a pK_{ESH} of 7.7.

Scheme 2: Kinetic Mechanism for Hydrolysis of *p*NP-TMP by ϵ186

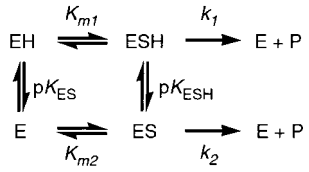

with an apparent pK_a of ~7.7, active in its deprotonated form. The solid line in Figure 5A represents the theoretical pH dependence according to the kinetic mechanism of Scheme 2 where $k_1 = 50$ min^{-1}, $k_2 = 400$ min^{-1}, and $pK_{ESH} = 7.75$. An interesting aspect of this pH dependence is that activity is not reduced to zero at pH <6.5. This suggests that deprotonation of the group that titrates with a pK_a of ~7.7 is not strictly necessary for activity, but contributes only an ~8-fold increase in k_{cat}. An alternate possibility is that the mechanism of *p*NP-TMP hydrolysis is fundamentally different at low and high pH values. These aspects are considered below in a detailed discussion of the mechanism.

DISCUSSION

The principal outcomes of this work are development of a convenient continuous spectrophotometric assay for measurement of the activity of the ϵ proofreading exonuclease and use of this assay to develop insights into how the enzyme works. The assay system, which may be more widely useful in studies of enzymes in this class, relies on release of *p*-nitrophenolate anion during ϵ- and ϵ186-catalyzed hydrolysis of the *p*-nitrophenyl ester of thymidine 5′-monophosphate (*p*NP-TMP) at pH 8.0 (Scheme 1).

Having an assay that measures hydrolase activity with a small nucleoside 5′-phosphodiester substrate at the active site of ϵ allows us to compare its hydrolysis with literature data on DNA (single-stranded or mismatched primer−template) substrates, and to use the results of recent structural studies (*25*, *29*) to develop mechanistic proposals to explain similari-

ties and differences. Here, we first verified that under the standard assay conditions, full-length ϵ and ϵ186 have comparable activities (k_{cat} and K_M) in hydrolysis of *p*NP-TMP. This confirms that the C-terminal domain of ϵ (residues 186−245) that interacts with α (*16*, *17*) has little direct influence on the chemistry that occurs at the active site of ϵ, and securely locates all residues directly involved in *p*NP-TMP hydrolase activity within the N-terminal ϵ186 domain.

The isolated ϵ186·θ complex also catalyzed the hydrolysis of *p*NP-TMP with kinetic parameters k_{cat} and K_M similar to those of ϵ186 itself; k_{cat} under the conditions that were used was reproducibly ~25% lower than for ϵ186. The role of θ in the pol III core is still uncertain. It is not required for the polymerase or exonuclease activities of the core or holoenzyme (*14*, *19*), and its gene could be inactivated without an apparent effect on viability or growth of *E. coli* (*38*). Association with θ was shown previously to stimulate ϵ 2−4-fold in removal of terminal nucleotides from primer−template or ssDNA substrates (*12*, *17*). These results suggest that this is probably not due to an effect on the structure of the active site of ϵ, but rather to participation of θ in a minor way in facilitating interaction of ϵ with the DNA substrate.

The pol III core (α·ϵ·θ complex) is isolable intact and appears to be quite stable to dissociation (*19*). We expected the ϵ·θ and ϵ186·θ complexes also to have low dissociation constants. It came as no surprise, therefore, that its interaction with θ stabilizes ϵ186 against thermal inactivation to a remarkable degree (Figure 2). This is also consistent with other observations. At high concentrations in phosphate buffer (pH 6.5), we observed that ϵ186 precipitated within minutes at 35 °C, which made it difficult to record high-resolution NMR spectra under optimal conditions (*18*). Although the θ subunit by itself is somewhat more stable under such conditions, much of its structure is quite flexible (*33*). In contrast, the ϵ186·θ complex is stable for at least 1 week at 30 °C, and preliminary NMR data indicate that the flexibility of θ in the complex is much reduced (*33*).

The activities of polymerase-associated proofreading 3′−5′ exonucleases have generally been measured using radiolabeled mismatched primer−template, partial duplex, or ssDNA substrates. These assays are cumbersome and somewhat irreproducible depending on the substrate that is used and batch-to-batch variations. Availability of a straightforward continuous spectrophotometric assay overcomes many of these difficulties. *p*NP-TMP has been used previously as a substrate for other phosphodiesterases (*39*), and there has been one report of its hydrolysis by a proofreading exonuclease. In 1964, Lehman and Richardson (*40*) demonstrated its hydrolysis by *E. coli* exonuclease II (exo II, the 3′−5′ exonuclease of pol I), where K_M = 6 mM and k_{cat} = 3.9 min^{-1}, with 7 mM Mg^{2+} at 37 °C and pH 9.2 (where it was maximally active). By comparison, our results with ϵ186 (K_M = 4 mM and k_{cat} = 19 min^{-1}, with 12 mM Mg^{2+} at 25 °C and pH 8.0) indicate that it is probably no more than 10-fold more active in Mg(II)-dependent *p*NP-TMP hydrolysis than is exo II (pol I), when the activity of each is measured at its optimum pH.

For both ϵ and pol I, there are substantial differences between the kinetic parameters for hydrolysis of *p*NP-TMP and those for oligonucleotide substrates. For example, k_{cat} values for ϵ acting on ssDNA at pH 7.5 (5 mM $MgCl_2$) have been estimated to be 12 000 min^{-1} (*32*), while the large proteolytic (Klenow) fragment of pol I has a k_{cat} value on ssDNA under similar conditions of ~50−70 min^{-1} (*30*). For pol I, Lehman and Richardson (*40*) reported ~20−60-fold lower K_M values for short oligonucleotide substrates [d(pT)$_n$T, n = 1−4], where the leaving group is a (oligo)-nucleotide 3′-OH rather than nitrophenolate; values of k_{cat} were 4−40-fold higher. For polynucleotide substrates, k_{cat} values were similar to those with short oligonucleotides, but values of K_m were more than 6 orders of magnitude lower, which reflects enhanced binding of the longer DNA chains also via the polymerase active site of pol I. Nevertheless, with the exception of the latter observation, which requires comparison of pol I with the pol III core or holoenzyme rather than with ϵ alone, indications are that the active sites and mechanisms of action of the exo II domain of pol I and ϵ are similar (*25*), except that ϵ exhibits considerably higher activity with DNA substrates.

As for hydrolysis of DNA substrates (*32*, *40*, *41*) promoted by both the Klenow fragment and ϵ, hydrolysis of *p*NP-TMP by ϵ186 depended on the presence of a divalent metal ion. While ϵ186 appears to be more active with Mn^{2+} than with Mg^{2+} under the conditions of the assay, further work is necessary to establish which of these (or other) metal ions is used in vivo and whether the same dependence is observed with DNA substrates. It is likely that the active site metal ions both exchange readily under the conditions of the assays, and we have also not yet determined, for example, by spectroscopic, kinetic, or crystallographic studies, whether either or both metal ions bind to ϵ186 in the absence of substrates or dNMP inhibitors.

The structure of the Klenow fragment has been determined at high resolution (*21*), and extensive crystallographic, mutagenesis, and kinetic studies have led to the proposal of a mechanism for its 3′−5′ exonuclease reaction (*29*, *41*, *42*). In the presence of substrate, its active site contains two divalent metal ions, where one (Me_A) is more extensively coordinated to protein ligands than the other (Me_B). Both metal ions are presumably Mg^{2+} in most of the kinetic studies, but crystal structures have Zn^{2+}, Mn^{2+}, or Mg^{2+} at the Me_A site. In the mechanism, one phosphate oxygen atom of the substrate bridges Me_A and Me_B, which polarizes it for in-line nucleophilic attack by hydroxide ion coordinated to Me_A. The 3′-oxygen of the ester coordinates to Me_B in the trigonal bipyramidal transition state, assisting the nucleotide 3′-OH in leaving. In the model, deprotonation of the Me_A-bound water (or hydroxide) is influenced by the presence, within H-bonding distance, of the OH group of Tyr497.

This general mechanism of substrate hydrolysis at a binuclear metal center, where a hydroxide ion coordinated to one metal ion is the nucleophile that attacks a substrate activated by the other, was proposed more than 20 years ago for the nickel metalloenzyme urease (*43*), partly on the basis of model studies of hydrolysis of phosphate and carboxylate esters and amides coordinated to substitution-inert metal ions such as Co(III) (*44*). Variations of this mechanism have since been found to apply to a large class of binuclear metallohydrolases (*45*).

As revealed by the crystal structure of the ϵ186·$Mn(II)_2$·TMP complex, the architecture of its active site is closely

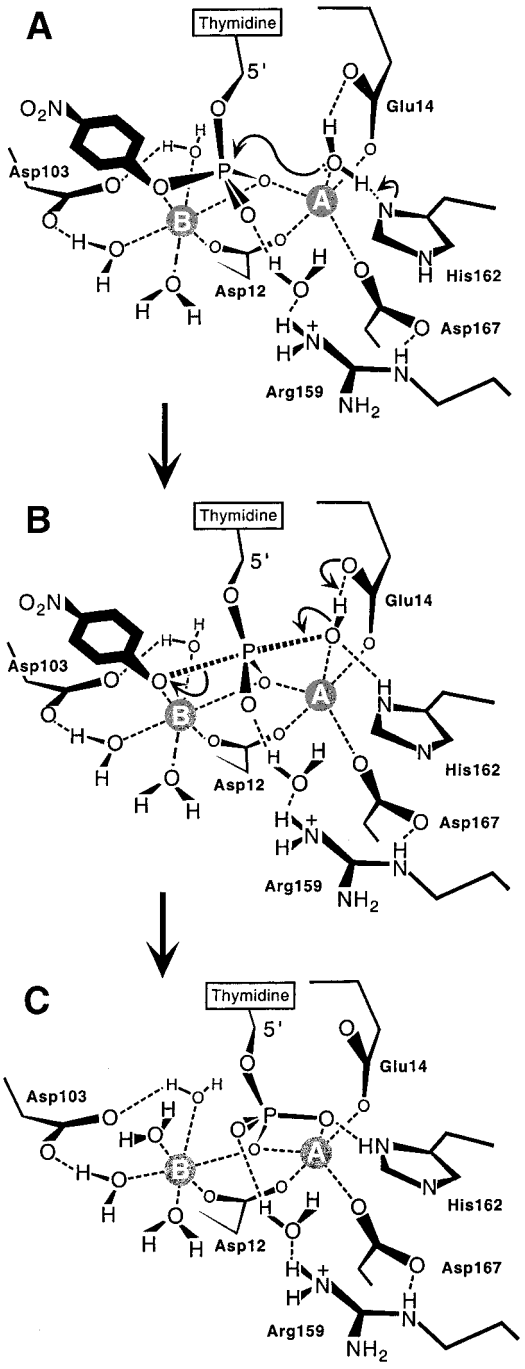

FIGURE 6: Proposal for the mechanism of hydrolysis of *p*NP-TMP by ϵ at high pH (>7). The structure of the enzyme−substrate complex (A) was modeled on the experimental structure (*25*) of the ϵ186·$Mn(II)_2$·TMP complex at pH 8.5 (PDB entry 1J53), while that of the enzyme−product complex (C) is based on a slightly different view of the structure (*25*) determined at pH 5.8 (PDB entry 1J54). A proposal for the structure of the phosphorane transition state (or intermediate) is shown in panel B.

related to that of pol I and other enzymes in this class (*25*), suggesting that the enzymes function by a similar mechanism. Catalysis by ϵ also involves the two metal ions in a binuclear center, and a histidine residue (His162) occupies the position of the active site Tyr497 in pol I. The binuclear Mn(II) center is coordinated to protein carboxylate ligands in the exo I, exo II, and exo IIIϵ motifs and to the 5′-phosphate of TMP. Shown in Figure 6 is a proposal for the mechanism of hydrolysis of *p*NP-TMP by ϵ that is consistent with the crystal structure of the ϵ186·$Mn(II)_2$·TMP complex at pH 8.5 (*25*) as well as data reported in this paper.

The higher activity of ϵ in hydrolysis of DNA substrates compared with that of *p*NP-TMP is not due to it being a highly processive enzyme. When it is not associated with α in the context of the holoenzyme (*20*), ϵ hydrolyzes only one (or a few) nucleotide(s) per binding event (*17*, *32*). Moreover, since *p*-nitrophenol is a stronger acid than the 3′-OH group at the end of a polynucleotide chain by a factor of $\sim 10^7$, it should be a very much better leaving group. Therefore, the natural DNA substrates must be substantially activated by a mechanism unavailable to *p*NP-TMP, and this would be true regardless of whether P−O bond breakage is the rate-determining step in the reaction.

One source of activation of natural DNA substrates is apparent in the mechanism in Figure 6, where the *p*-nitrophenolate leaving group of *p*NP-TMP is shown coordinated to Mn_B, in the orientation required for its concerted elimination via a S_N2 reaction at the 5′-phosphate. The active site of ϵ is presumably designed to accommodate the deoxyribose moiety of the penultimate nucleotide in this position, and there is no obvious contact that would encourage *p*-nitrophenol to occupy this site. Moreover, in parallel with its low proton affinity due to electron withdrawal by the *p*-NO_2 group, the oxygen atom of the ester would be expected to be a very feebly coordinating ligand. Thus, it is very likely that the *p*-nitrophenolate leaving group spends only a small fraction of time in the orientation required for *p*NP-TMP hydrolysis by a concerted S_N2 reaction. The situation with natural polynucleotide substrates is very different. The leaving group is a long DNA strand which, by analogy with pol I (*42*, *46*, *47*), must interact extensively with other residues to position the leaving group precisely in an orientation that favors P−O bond breakage, and this orientational effect is likely to be one of the most important contributors to catalytic efficiency (*25*).

The observation that the K_i for competitive inhibition of ϵ186-promoted *p*NP-TMP hydrolysis by the product TMP is ~250-fold lower than the K_M for the substrate is also explained by direct coordination of the substrate (and product) to an active site metal ion as shown in Figure 6. At pH 8, TMP is a dianion while the substrate is a monoanion, so the latter would be expected to bind much less avidly to the binuclear metal center. This difference in K_i for product compared with K_M for substrate is also reflected in the pK_a of His162, which is 7.7 in the ϵ186·*p*NP-TMP complex (see below) and ~6.5 in the complex with TMP under the conditions of the crystallographic studies (*25*).

The most obvious difference between the active sites of pol I and ϵ186 is that Tyr497 in the exo III motif of pol I is replaced with His162 in the exo IIIϵ motif of ϵ, where it is ideally positioned to act as a general base to deprotonate a water molecule coordinated to Mn_A. While this alone may account for the higher *p*NP-TMP hydrolase activity of ϵ in comparison with that of pol I, it is unlikely to do so in the case of DNA substrates because the comparably (or more) active exonuclease domains of the T4 (*48*, *49*) and T7 (*50*, *51*) DNA polymerases both have tyrosines at equivalent positions (*23*, *52*, *53*). On the other hand, a His162 to Tyr mutant of ϵ has been isolated from a screen for mutator mutations in *dnaQ* (*54*), which suggests that tyrosine and histidine are not interchangeable at this position in ϵ.

Support for the proposition that His162, in its deprotonated form, is involved in ϵ-catalyzed *p*NP-TMP hydrolysis comes from examination of the pH dependence of k_{cat} and K_M (Figure 5). These profiles are both apparently very simple, in accord with the kinetic mechanism in Scheme 2. We are now able to interpret these data in terms of the structure of the active site to develop further insights into the mechanism by which ϵ promotes the hydrolysis of *p*NP-TMP (Figure 6). The crystal structures at low and high pH (*25*) differ in the way TMP is bound at the active site so that the high-pH structure appears to mimic the Michaelis complex (Figure 6A) while the low-pH structure mimics the first-formed product (Figure 6C).

Values of K_M were found to be essentially independent of pH in the range of 6.5−8.5. Since $K_{m1} \approx K_{m2}$ (Scheme 2), it follows that $pK_{EH} \approx pK_{ESH}$, so binding of the substrate has very little influence on the pK_a of the titratable group at the active site. This is in accord with the mechanism, since the negative charge on the 5′-phosphate of the substrate is effectively neutralized by its coordination to the binuclear metal center. At pH >8.5, there is a suggestion of an increase in K_M (Figure 5B), which very likely reflects the effect of deprotonation of the side chain of Arg159 on substrate binding. The guanidinium group of Arg159 forms a water-mediated hydrogen bond with the phosphoryl oxygen of TMP in the crystal structure. It is proposed in Figure 6 to do likewise in the complex with *p*NP-TMP. The role of Arg159 in hydrolysis of DNA substrates, as opposed to *p*NP-TMP, is likely to be more profound, because model building strongly suggests it would interact directly with the phosphate group of the penultimate nucleotide, thereby making a larger contribution to substrate binding when the substrate is a polynucleotide (*25*).

The pH−k_{cat} profile for Mn(II)-promoted *p*NP-TMP hydrolysis by ϵ186 (Figure 5A) exhibited an apparently simple dependence on a group with a pK_a of 7.7, which we propose to be His162 or, more precisely, the Mn_A·OH_2·His162 array (see below). A most surprising aspect is that ϵ186 retains substantial activity toward *p*NP-TMP at low pH values where this group is fully protonated (see Figure 5A and Scheme 2; $k_1 \sim 50$ min^{-1} vs $k_2 = 400$ min^{-1}). As discussed below, this probably indicates a fundamental difference between the mechanisms used by ϵ for *p*NP-TMP hydrolysis at high and low pH values.

At high pH values, the dependence of k_{cat} on pH is qualitatively similar to that for hydrolysis of oligonucleotide substrates by the 3′−5′ exonuclease of pol I, where k_{cat} reflects the ionization of a group with a pK_a of ∼9.8, active in its deprotonated form (*30*). There has been some debate about whether this pK_a should be assigned to Tyr497 or the nucleophilic Mg_A-coordinated water and whether Tyr497 serves as a general base or simply to orient the nucleophile (*30*, *41*, *55*). Since the pK_a values of tyrosine and Mg(II)·OH_2 in isolation are similar and near 9.8, the distinction between the two possibilities reflects only the position of a proton between the two groups in the deprotonated active site and is not meaningful or significant (Scheme 3A). Rather, the kinetically determined pK_a is that of the protonated form of the hydrogen-bonded Mg_A·OH_2·Tyr497 array, regardless of the position from which the proton is actually removed.

The same is to a lesser extent true for the protonated Mn_A·OH_2·His162 moiety in ϵ186, where its kinetically determined

Scheme 3

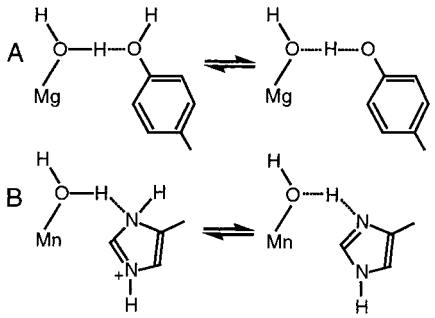

pK_a of 7.7 is between that expected for an isolated protonated imidazole (∼7) and Mn(II)-coordinated water (∼9 or ∼10) (*56*). The effect of the hydrogen bond between the two groups (Scheme 3B) can be looked upon as either raising the pK_a of the imidazole of His162 or lowering that of the coordinated water. Certainly, during *p*NP-TMP hydrolysis, it would be expected that complete transfer of the proton to His162 would create the Mn_A-coordinated hydroxide nucleophile that attacks the 5′-phosphate of the substrate from the back side (*57*), resulting in inversion about phosphorus through a trigonal bipyramidal (five-coordinate phosphorane) transition state (Figure 6B), ultimately to produce a TMP complex that is very similar to that seen in the low-pH crystal structure (Figure 6C). The possibility that the phosphorane may be an intermediate rather than a transition state, with a lifetime sufficiently long to allow it to deprotonate and/or undergo structural changes, should not be discounted. A similar species has been detected as a short-lived intermediate during hydrolysis of Co(III)-coordinated *p*-nitrophenyl phosphate following intramolecular attack of a cis-coordinated hydroxide nucleophile (*58*). If such an intermediate were to rearrange before the leaving group were expelled, the requirement in an S_N2 reaction for concerted in-line nucleophilic attack from the back side of the phosphate and displacement of the leaving group from the front (*57*) could be relaxed.

It is pertinent to consider the role of Glu14 (and the corresponding residue Glu357 in pol I), one of whose carboxylate oxygens is a ligand to Mn_A while the other forms a second hydrogen bond to the nucleophilic water molecule. Mutational analysis of pol I suggested that the role of Glu357 in Me_A binding is less important than some other (unidentified) aspect of its function (*30*). Since it thus appears that Glu357 in pol I does not lose too much electron density to the metal center, both it and Glu14 in ϵ are therefore estimated to have pK_a values of ∼3−4. Now, the phosphorane transition state derived from the 5′-phosphate of *p*NP-TMP is likely to have a somewhat lower pK_a than TMP itself (i.e., 6.5) because of extensive charge neutralization by its coordination to the binuclear Mn(II) center. Its pK_a is thus well-matched to that of Glu14, which is therefore likely to accept a further proton from the transition state (or intermediate), driving its collapse in the direction that would lead to elimination of the leaving group. Because Glu14 is such a weak base, the driving force provided thus to the reaction when the leaving group is *p*-nitrophenolate is likely to be modest. With a poorer leaving group like a deoxyribose 3′-OH, this second proton transfer is likely to be much more significant.

Now consider the need to protonate the leaving group. Because the pK_a of *p*-nitrophenol is 7, there is no advantage in providing a proton source to facilitate its leaving at high pH. With a DNA substrate, however, a general acid would clearly be required to protonate the leaving polynucleotide 3′-OH. The only appropriately placed active site acid is one of the Mn_B-coordinated water molecules H-bonded to Asp103 (Figure 6). Although their pK_a values will not be lowered much as a result of their interaction with Asp103, they will still have very much lower proton affinities than the deprotonated deoxyribose 3′-OH.

We now turn briefly to the mechanism of ϵ-promoted hydrolysis of *p*NP-TMP at (low) pH values where the Mn_A·OH_2·His162 array is fully protonated. The mechanism is unlikely to be similar to that at high pH (Figure 6); because of its coordination to Mn_A, the remaining base, Glu14, is too weak to deprotonate the Mn_A-coordinated water and, in the absence of a base to deprotonate it, the coordinated water would be a far too weak nucleophile to account for the high residual activity of ϵ.

To explain *p*NP-TMP hydrolase activity at low pH, we therefore need to invoke fundamentally different mechanisms that may be more closely related to those used by some acid phosphatases (*59*). For example, the leaving group could now occupy the position of the phosphoryl oxygen in Figure 6, and a Mn_B-coordinated hydroxide ion could act as a nucleophile. Although this plausibly explains the low-pH activity of ϵ on a small synthetic substrate like *p*NP-TMP, it is unlikely to be feasible with natural DNA substrates because of the more extensive contacts polynucleotide chains must make with residues around the active site. For example, model building based on the structures of oligonucleotide complexes with the proofreading active site of pol I suggests that the 5′-phosphate of the penultimate dNMP of DNA substrates has an ionic interaction with the side chain of Arg159 in ϵ (*25*). This would preclude binding of the phosphate group of the terminal dNMP in the orientation required for such a mechanism to operate with DNA substrates at low pH. At the moment, there is no detailed information available about the pH dependence of DNA hydrolysis by ϵ.

In conclusion, we note that the mechanism proposed in Figure 6 and the likelihood of a different mechanism operating with *p*NP-TMP as the substrate at low pH give rise to many further hypotheses that may be tested using site-directed mutagenesis, structure determination, and mechanistic enzymology. For example, whether pH-dependent differences occur in the structures of complexes of ϵ186 with *p*NP-TMP or other synthetic nucleoside 5′-phosphoester substrates and whether they might also occur with oligonucleotide substrates are questions that obviously require further investigation.

ACKNOWLEDGMENT

We are grateful to Dr. Harrison Echols for provision of pNS360, to Carl Braybrook for ESI-MS, and to James Kelly and Tony Herlt for help with HPLC. We are especially grateful to Professor Alan Sargeson for his critical comments.

SUPPORTING INFORMATION AVAILABLE

Details of methods used for overexpression of ϵ and ϵ186 and for purification of ϵ, ϵ186, θ, and the ϵ186·θ complex. This material is available free of charge via the Internet at http://pubs.acs.org.

REFERENCES

1. Herendeen, D. R., and Kelly, T. J. (1996) *Cell 84*, 5−8.
2. Kelman, Z., and O'Donnell, M. (1995) *Annu. Rev. Biochem. 64*, 171−200.
3. Baker, T. A., and Bell, S. P. (1998) *Cell 92*, 295−305.
4. Degnen, G. E., and Cox, E. C. (1974) *J. Bacteriol. 117*, 477−487.
5. Horiuchi, T., Maki, H., and Sekiguchi, M. (1978) *Mol. Gen. Genet. 163*, 277−283.
6. Horiuchi, T., Maki, H., Maruyama, M., and Sekiguchi, M. (1981) *Proc. Natl. Acad. Sci. U.S.A. 78*, 3770−3774.
7. Cox, E. C., and Horner, D. L. (1983) *Proc. Natl. Acad. Sci. U.S.A. 80*, 2295−2299.
8. Echols, H., Lu, C., and Burgers, P. M. J. (1983) *Proc. Natl. Acad. Sci. U.S.A. 80*, 2189−2192.
9. Scheuermann, R., Tam, S., Burgers, P. M. J., Lu, C., and Echols, H. (1983) *Proc. Natl. Acad. Sci. U.S.A. 80*, 7085−7089.
10. Maki, H., Horiuchi, T., and Sekiguchi, M. (1983) *Proc. Natl. Acad. Sci. U.S.A. 80*, 7137−7141.
11. Scheuermann, R. H., and Echols, H. (1984) *Proc. Natl. Acad. Sci. U.S.A. 81*, 7747−7751.
12. Studwell-Vaughan, P. S., and O'Donnell, M. (1993) *J. Biol. Chem. 268*, 11785−11791.
13. Kunkel, T. A. (1988) *Cell 53*, 837−840.
14. Studwell, P. S., and O'Donnell, M. (1990) *J. Biol. Chem. 265*, 1171−1178.
15. Kunkel, T. A., and Bebenek, K. (2000) *Annu. Rev. Biochem. 69*, 497−529.
16. Taft-Benz, S. A., and Schaaper, R. M. (1999) *J. Bacteriol. 181*, 2963−2965.
17. Perrino, F. W., Harvey, S., and McNeill, S. M. (1999) *Biochemistry 38*, 16001−16009.
18. Hamdan, S., Brown, S. E., Thompson, P. R., Yang, J. Y., Carr, P. D., Ollis, D. L., Otting, G., and Dixon, N. E. (2000) *J. Struct. Biol. 131*, 164−169.
19. Maki, H., and Kornberg, A. (1987) *Proc. Natl. Acad. Sci. U.S.A. 84*, 4389−4392.
20. Reems, J. A., Griep, M. A., and McHenry, C. S. (1991) *J. Biol. Chem. 266*, 4878−4882.
21. Ollis, D. L., Brick, P., Hamlin, R., Xuong, N. G., and Steitz, T. A. (1985) *Nature 313*, 762−766.
22. Morrison, A., Bell, J. B., Kunkel, T. A., and Sugino, A. (1991) *Proc. Natl. Acad. Sci. U.S.A. 88*, 9473−9477.
23. Blanco, L., Bernad, A., and Salas, M. (1992) *Gene 112*, 139−144.
24. Barnes, M. H., Spacciapoli, P., Li, D. H., and Brown, N. C. (1995) *Gene 165*, 45−50.
25. Hamdan, S., Carr, P. D., Brown, S. E., Ollis, D. L., and Dixon, N. E. (2002) *Structure 10* (in press).
26. Fijalkowska, I. J., and Schaaper, R. M. (1996) *Proc. Natl. Acad. Sci. U.S.A. 93*, 2856−2861.
27. Taft-Benz, S. A., and Schaaper, R. M. (1998) *Nucleic Acids Res. 26*, 4005−4011.
28. Jonczyk, P., Nowicka, A., Fijalkowska, I. J., Schaaper, R. M., and Ciesla, Z. (1998) *J. Bacteriol. 180*, 1563−1566.
29. DeRose, E. F., Li, D., Darden, T., Harvey, S., Perrino, F. W., Schaaper, R. M., and London, R. E. (2002) *Biochemistry 41*, 94−110.
30. Derbyshire, V., Grindley, N. D. F., and Joyce, C. M. (1991) *EMBO J. 10*, 17−24.
31. Brenowitz, S., Kwack, S., Goodman, M. F., O'Donnell, M., and Echols, H. (1991) *J. Biol. Chem. 266*, 7888−7892.
32. Miller, H., and Perrino, F. W. (1996) *Biochemistry 35*, 12919−12925.
33. Keniry, M. A., Berthon, H. A., Yang, J. Y., Miles, C. S., and Dixon, N. E. (2000) *Protein Sci. 9*, 721−733.
34. Gill, S. C., and Von Hippel, P. H. (1989) *Anal. Biochem. 182*, 319−326.

35. Smith, M., and Khorana, H. G. (1963) *Methods Enzymol. 6*, 645−669.
36. Kuzmic, P. (1996) *Anal. Biochem. 237*, 260−273.
37. Thompson, P. R. (1992) Ph.D. Thesis, Australian National University, Canberra, Australia.
38. Slater, S. C., Lifsics, M. R., O'Donnell, M., and Maurer, R. (1994) *J. Bacteriol. 176*, 815−821.
39. Razzell, W. E. (1963) *Methods Enzymol. 6*, 236−258.
40. Lehman, I. R., and Richardson, C. C. (1964) *J. Biol. Chem. 239*, 233−241.
41. Beese, L. S., and Steitz, T. A. (1991) *EMBO J. 10*, 25−33.
42. Brautigam, C. A., and Steitz, T. A. (1998) *J. Mol. Biol. 277*, 363−377.
43. Dixon, N. E., Riddles, P. W., Gazzola, C., Blakeley, R. L., and Zerner, B. (1980) *Can. J. Biochem. 58*, 1335−1344.
44. Dixon, N. E., and Sargeson, A. M. (1983) in *Zinc Enzymes* (Spiro, T. G., Ed.) pp 253−352, John Wiley and Sons, New York.
45. Wilcox, D. E. (1996) *Chem. Rev. 96*, 2435−2458.
46. Beese, L. S., Derbyshire, V., and Steitz, T. A. (1993) *Science 260*, 352−355.
47. Brautigam, C. A., Sun, S., Piccirilli, J. A., and Steitz, T. A. (1999) *Biochemistry 38*, 696−704.
48. Capson, T. L., Peliska, J. A., Fenn Kaboord, B., West Frey, M., Lively, C., Dahlberg, M., and Benkovic, S. J. (1992) *Biochemistry 31*, 10984−10994.
49. Reddy, M. K., Weitzel, S. E., and Von Hippel, P. H. (1992) *J. Biol. Chem. 267*, 14157−14166.
50. Donlin, M. J., Patel, S. S., and Johnson, K. A. (1991) *Biochemistry 30*, 538−546.
51. Johnson, K. A. (1993) *Annu. Rev. Biochem. 62*, 685−713.
52. Wang, J., Yu, P., Lin, T. C., Konigsberg, W. H., and Steitz, T. A. (1996) *Biochemistry 35*, 8110−8119.
53. Doublié, S., Tabor, S., Long, A. M., Richardson, C. C., and Ellenberger, T. (1998) *Nature 391*, 251−258.
54. Strauss, B. S., Sagher, D., and Acharya, S. (1997) *Nucleic Acids Res. 25*, 806−813.
55. Freemont, P. S., Friedman, J. M., Beese, L. S., Sanderson, M. R., and Steitz, T. A. (1988) *Proc. Natl. Acad. Sci. U.S.A. 85*, 8924−8928.
56. Basolo, F., and Pearson, R. G. (1967) *Mechanisms of Inorganic Reactions*, 2nd ed., John Wiley and Sons, New York.
57. Knowles, J. R. (1980) *Annu. Rev. Biochem. 49*, 877−919.
58. Jones, D. R., Lindoy, L. F., and Sargeson, A. M. (1983) *J. Am. Chem. Soc. 105*, 7327−7336.
59. Klabunde, T., Strater, N., Frohlich, R., Witzel, H., and Krebs, B. (1996) *J. Mol. Biol. 259*, 737−748.

BI0159480